Active sites in Cu-SSZ-13 deNOx catalyst under reaction conditions: a XAS/XES perspective

2016 J. Phys.: Conf. Ser. 712 012041

(http://iopscience.iop.org/1742-6596/712/1/012041)

Journal of Physics: Conference Series **712** (2016) 012041 doi:10.1088/1742-6596/712/1/012041

Active sites in Cu-SSZ-13 deNO$_x$ catalyst under reaction conditions: a XAS/XES perspective

Kirill A Lomachenko[1,2,*], Elisa Borfecchia[2], Silvia Bordiga[2], Alexander V Soldatov[1], Pablo Beato[3] and Carlo Lamberti[1,2,*]

[1] Southern Federal University, Zorge street 5, 344090 Rostov-on-Don, Russia
[2] Department of Chemistry and INSTM Reference Center, University of Turin, via P. Giuria 7, 10125 Turin, Italy
[3] Haldor Topsøe A/S, Nymøllevej 55, 2800 Kgs. Lyngby, Denmark

E-mail: carlo.lamberti@unito.it, kirlom@gmail.com

Abstract. Cu-SSZ-13 is a highly active catalyst for the NH_3-assisted selective catalytic reduction (SCR) of the harmful nitrogen oxides (NO_x, x=1, 2). Since the catalytically active sites for this reaction are mainly represented by isolated Cu ions incorporated into the zeolitic framework, element-selective studies of Cu local environment are crucial to fully understand the enhanced catalytic properties of this material. Herein, we highlight the recent advances in the characterization of the most abundant Cu-sites in Cu-SSZ-13 upon different reaction-relevant conditions made employing XAS and XES spectroscopies, complemented by computational analysis. A concise review of the most relevant literature is also presented.

1. Introduction

The Cu-exchanged form of the novel SSZ-13 zeolite, with CHA framework and high Si/Al ratio, is attracting a lot of attention due to its outstanding performance in NH_3-assisted selective catalytic reduction (SCR) of NO_x gases contained in the exhaust fumes from cars and industrial plants. Although H-SSZ-13 was first synthesized in 1985 [1] it was demonstrated that Cu-SSZ-13 outperforms other SCR catalysts (namely Cu-ZSM-5 and Cu-β zeolites) in terms of activity and hydrothermal stability only in the late 2000s [2, 3]. In order to explain such behavior and to develop the NH_3-based SCR reaction mechanism many studies were performed by research groups all over the world involving a very broad range of characterization techniques, such as FTIR, UV-Vis, EPR, NMR, XRD and others, as recently reviewed in [4]. Among them, X-ray spectroscopy (both absorption and emission) is particularly useful due to its element selectivity, since the active sites of SCR reaction in Cu-SSZ-13 are highly diluted Cu ions hosted in the cavities of the zeolite framework. Careful analysis of EXAFS, XANES and XES spectra, often assisted by advanced DFT calculations, yields detailed information on the local environment and oxidation state of Cu centers in different reaction conditions [4-9]. *In situ* and *operando* studies, possible due to the high penetration depth of hard X-rays (around 9 keV, corresponding to the Cu K-edge), provide the means to answer "chemical questions" concerning the reactivity of the Cu species towards particular gases at given temperatures, which is crucial for determining different steps of the reaction mechanism [10-12].

However, most of XAS and XES studies are feasible only exploiting synchrotron sources, which obviously makes these techniques much less common compared to the standard laboratory

characterization methods. Therefore, the following review of the advances made in the understanding of the Cu-SSZ-13 chemistry by means of XAS and XES will be useful not only for the X-ray spectroscopy community, but also for the broad chemical audience, as a demonstration of the power of these techniques applied to the study of metal-exchanged porous catalysts under reaction conditions.

2. Exploring the activation process

The structure of natural copper-exchanged CHA framework has been known for a long time from single crystal diffraction studies [13]. The structure of Cu-SSZ-13 is similar, but with a lower Al and Cu content. It is composed of double six-membered rings (6-rings) connected in an AABBCC sequence forming cavities with eight-membered windows (8-rings) (figure 1).

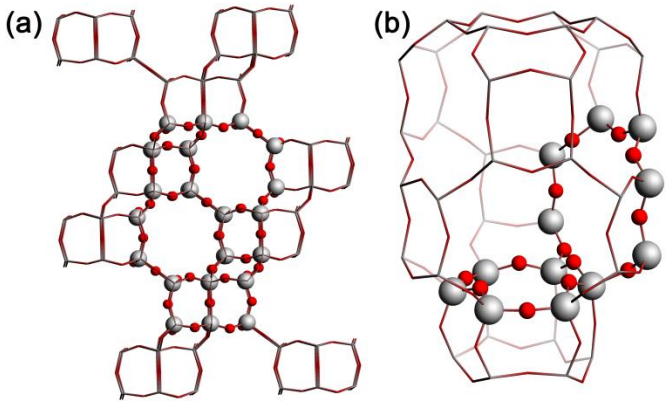

Figure 1. (a) Fragment of CHA framework with the atoms forming the large cavity highlighted; (b) close-up of the large CHA cavity showing 6- and 8-membered rings, which are reported to be the most probable hosts for Cu ions. Color code: Si – gray, O – red.

After the discovery of the outstanding catalytic properties of synthetic Cu-SSZ-13 [14], the focus of the structural investigations was gradually shifted from the framework to the location of the isolated Cu ions in the hydrated and thermally activated material, which were suggested to be the active sites of the SCR reaction. One of the first studies, carried out by Fickel and Lobo demonstrated that the Cu ions tend to occupy the centers of the 6-rings [15]. Since every 6-ring is likely to have one negatively charged tetrahedral unit with Al substituting Si, the authors admitted that Cu cations are expected to be shifted towards it from the center of the ring. However, XRD refinement was always converging to central position due to the lack of structural contrast. Nonetheless, it was possible to detect that, being always "projected" on the center of the 6-ring, the Cu ions were gradually approaching its plane upon calcination. The authors suggested that this effect may take place due to the dehydration of the Cu ions.

In a subsequent work Korhonen *et al.* presented Cu K-edge EXAFS data for both calcined and as-synthesized (hydrated) Cu-SSZ-13 [16] and performed a fit using as a model a theoretical structure of Cu in the 6-ring reported earlier (figure 2a) [17].

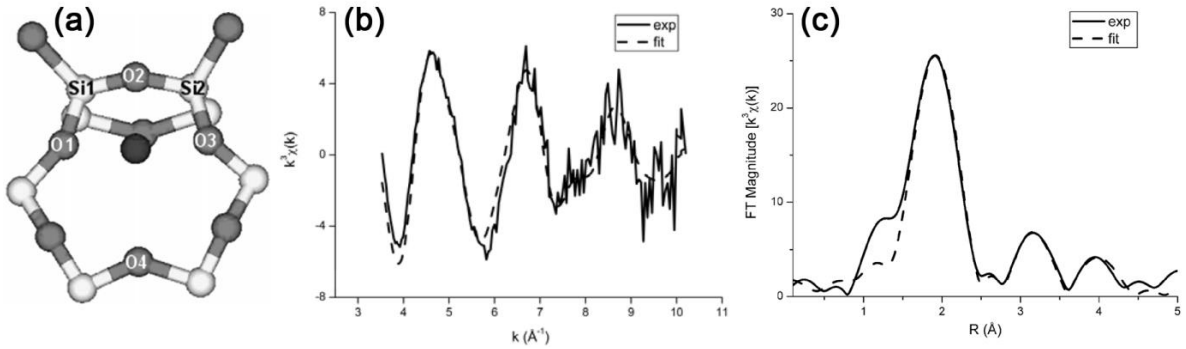

Figure 2. (a) DFT model of Cu in SSZ-13 6-ring employed for the fitting; (b) experimental and fitted k^3-weighted EXAFS signal of the Cu-SSZ-13 calcined at 500 °C and (c) the modulus of its Fourier transform corrected by Cu-O phase. Adapted with permission from Korhonen *et al.* [16]. Copyright (2011) The Royal Society of Chemistry.

The fit resulted in adequate agreement with the experiment, confirming that Cu is indeed shifted from the center of the 6-ring (figure 2b,c). The very substantial displacement of one of the oxygens in the 6-ring from the initial position during fitting was explained by the lower degree of deformation of the ring compared to the one predicted by DFT. First shell coordination numbers were determined as 4 for hydrated material and 3.2 for the calcined one. Presented XANES results also indicated the decrease of coordination upon dehydration due to the decrease of the main maximum (the white line). Later, the shift of the Cu ion from the center of the 6-ring was also confirmed by Deka *et al.*, by means of XANES simulations [18]. Calculated spectrum of the model with Cu placed off-axis resulted in a much better agreement with the experimental data compared to the centered model.

Hydration issue was raised in more detail in the work by McEwen *et al.* where it was demonstrated that Cu K-edge XANES spectrum of the as-synthesized Cu-SSZ-13 zeolite is very similar to the one of aqueous solution of Cu ions [19]. This was further confirmed by Borfecchia *et al.*, who presented also a comparison of the EXAFS data for these two cases [6]. High degree of similarity of both XANES and EXAFS data suggests that as long as the zeolite is exposed to air at room temperature, copper is covered by a shell of water molecules. Such shielding explains the lack of the framework contribution to the EXAFS data of the hydrated material and confirms the initial hypothesis of Fickel and Lobo [15]. At the same time, a substitution of one H_2O molecule by OH^- group cannot be excluded since these species are hardly distinguishable in EXAFS.

One of the most extensive spectroscopic studies of the activated Cu-SSZ-13 to date was carried out by Borfecchia *et al.* [6]. EXAFS-optimized experimental setup and rather high copper content in the sample (Cu/Al=0.44, Si/Al=13.1) allowed to achieve a very good data quality paving the way to a detailed quantitative analysis. Comparison of both XANES and EXAFS spectra of hydrated material with the data for the zeolite activated in oxygen and in helium revealed the significant differences of these three states (figure 3).

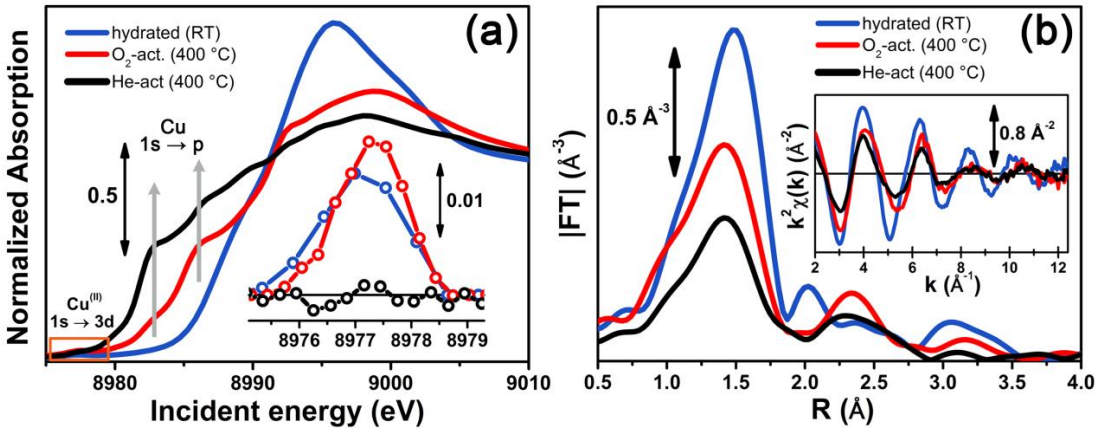

Figure 3. *In situ* static XAS data of the hydrated (RT), O_2-activated and He-activated (400 °C) Cu-SSZ-13 catalyst. (a) Cu K-edge XANES spectra; the inset shows the background-subtracted pre-edge peak highlighted by the orange box in the main panel. (b) Magnitude of the phase-uncorrected FT EXAFS spectra, obtained by transforming in the (2.4–12.4) $Å^{-1}$ range the k^2-weighted $\chi(k)$ curves reported in the inset. Adapted with permission from Borfecchia *et al.* [6]. Copyright (2015) The Royal Society of Chemistry.

It was confirmed that, upon heating in O_2, Cu(II) centers undergo progressive dehydration, while interacting more closely with the framework, with no significant modification of their oxidation state. Features typical for Cu(II) in low-symmetry environment were observed in XANES (figure 3a), while EXAFS witnessed the marked decrease of the first shell intensity due to the loss of the coordinated water molecules (figure 3b). Similar evolution of the XANES spectra upon activation in O_2 was reported also by Kwak *et al.* [20]. Conversely, as already observed for other zeolitic frameworks [21-28], upon activation in vacuum or in inert atmosphere (e.g. helium) the Cu oxidation state did change to +1, as

evidenced by the disappearance of 1s→3d transition (figure 3a, inset) and by the additional redshift of the edge. Most interestingly, high-quality EXAFS data reveal that the coordination of Cu upon He-activation was further decreased compared to the activation in O_2. Coupled with the observation that the reduction in He flow appears only at high temperature (T>250 °C), while at lower T the evolution of the spectra is identical to the O_2-activation case, it indicates that a charged extra-ligand is still coordinated to Cu even at high temperature in case of O_2-activation.

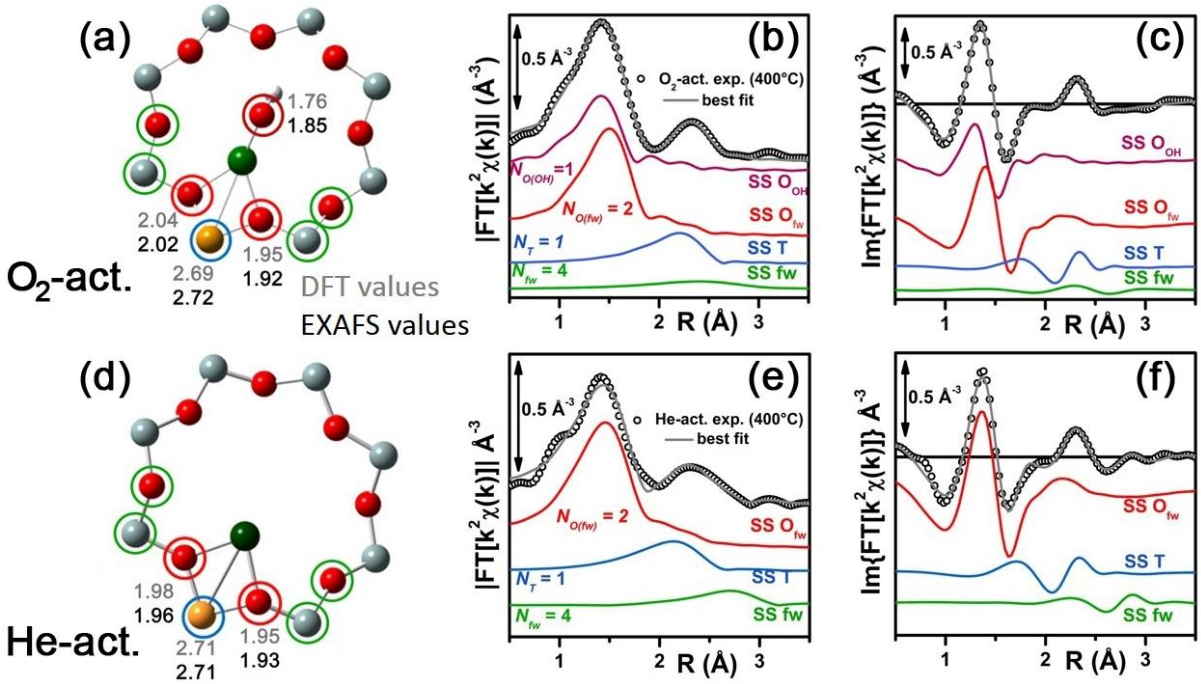

Figure 4. (a) DFT-optimized model of Cu in 8-ring that yielded the best agreement with the EXAFS data for the O_2-activated Cu-SSZ-13. Atom color code: Cu – green; H – white; O – red; Al – orange, Si – gray; Distances from Cu to the neighboring atoms are given in Å in grey (DFT values) and black (EXAFS values). Colored circles highlight the different coordination shells included in the fitting model; (b and c) experimental EXAFS spectrum of the O_2-activated Cu-SSZ-13 and corresponding best fit performed with the model from panel (a); modulus and imaginary part of the FT are shown in panels (b) and (c) respectively, together with the contributions of different shells, drawn with the same color code as in part (a) and translated vertically for the sake of clarity. (d, e, f) theoretical and experimental data for the case of He-activated Cu-SSZ-13, analogous to (a, b, c), respectively. Adapted with permission from Borfecchia *et al.* [6]. Copyright (2015) The Royal Society of Chemistry.

The authors have further tested this hypothesis by performing a set of DFT simulations of Cu ions in different locations in the framework and using the resulting structures as input for EXAFS fits and XANES and XES simulations. The best overall agreement with the experimental data was obtained for the models of Cu in the 8-ring. While in case of He-activation it was a bare Cu(I) cation (figure 4 d-f), after O_2-activation the OH^- ligand was found to be coordinated to the Cu(II) ion (figure 4 a-c), confirming the first assignment of the ν(OH) stretching mode at 3657 cm^{-1}, done by Giordanino *et al.* [29]. Interestingly, the seeming mismatch between the DFT and EXAFS data observed in the pioneering XAS work by Korhonen *et al.* might be explained. It appeared that the dramatic elongation of the distance between Cu and the "opposite" oxygen in the 6-ring observed by EXAFS led to an antiphase effect, which made the results of the fits in the 8-ring and in 6-ring very similar. Although the presence of the destructive interference between EXAFS paths cannot be automatically considered as a sign of fitting problem being sometimes a characteristic feature of the material, more careful analysis allowed to state that in this case it was a purely mathematical effect and the fit of the $Cu^{2+}(OH)^-$ structure in 8-

ring was much more robust. The presence of the OH^- groups coordinated to Cu was further supported by the FTIR results presented in the same publication [6] and confirmed by the EPR analysis of Godiksen *et al.* [30], while the Cu ions in the 8-ring position were detected also by high-resolution X-ray diffraction by Andersen *et al.* [31].

One of the highly debated questions in the Cu-zeolites community is the possibility to form small Cu oxo-clusters, usually dimers, inside the zeolitic pores under certain conditions. Detection of such species was reported in many studies [32-39]. However, generally the authors clearly state, that these are minority species. Such conclusion was reached, e.g. by Woertnik *et al.*, by means of resonant Raman for ZSM-5 [38] and by Godiksen *et al.* by EPR for SSZ-13 [30]. Since EXAFS always delivers the average picture, such low-abundance species are beyond the detection limit of this technique and the possibility of their existence cannot be neither ruled out nor confirmed from EXAFS data. Conversely, having Cu oxo-clusters as dominant species in Cu-SSZ-13 is very unlikely. In principle, it may be possible to imagine a hypothetic structure of a dimer o trimer, where several scattering paths cancel each other due to the antiphase effect and yield an EXAFS pattern with Cu-Cu contribution at around 2.3 Å (phase uncorrected) compatible with experimental data. However for Cu-SSZ-13, to the best of our knowledge, no comprehensive proof constituting a thorough EXAFS analysis complemented by other spectroscopic techniques (XANES, XES, UV-Vis) and theoretical calculations to support this argument has been presented so far. Contrarily, it was demonstrated that the feature at around 2.3 Å could be fitted very well considering the scattering from the framework Al in much simpler models with isolated Cu ions. DFT calculations based on these structural models were able to reproduce also the Cu K-edge XANES and Cu valence-to-core XES spectra. Being in agreement also with UV-Vis data, these structural models seem much more convincing as dominant species in Cu-SSZ-13 [6, 16, 18, 29].

3. Understanding the SCR mechanism

Since one of the most important goals of the Cu-SSZ-13 characterization is the understanding of the SCR reaction mechanism, a lot of efforts were invested into measuring X-ray absorption and emission spectra of this material in different reaction-relevant conditions. In the whole variety of the performed experiments, two major approaches can be distinguished. One comprises the experiments in truly *operando* conditions, when the sample is exposed to the complete reaction mixture (including NO, NH_3, O_2, He, H_2O, in some studies also NO_2 and CO_2) under controlled temperature. Most often such studies are performed in plug-flow reactors, such as the one described in the work of Kispersky *et al.* [40].

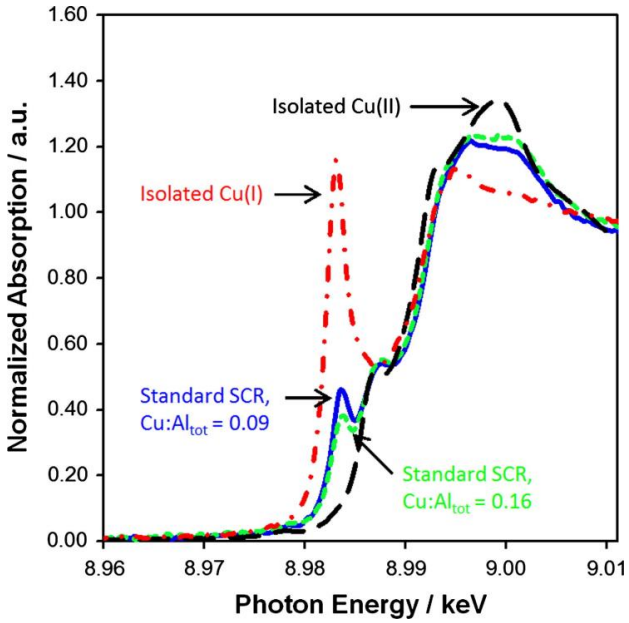

Figure 5. *Operando* Cu K-edge XANES spectra of Cu-SSZ-13 samples with Cu:Al ratio of 0.09 and 0.16 under standard SCR reaction conditions compared with the spectra of Cu-SSZ-13 with Cu:Al ratio of 0.02 collected upon the reaction with 1000 ppm NH_3 + 1000 ppm NO (isolated Cu(I)) and calcination in 10% O_2 (isolated Cu(II) references), both at 200 °C. The standard SCR conditions used were 320 ppm NO, 320 ppm NH_3, 10% O_2, 8% CO_2, 6% H_2O, and balance helium at 180 °C. Reproduced with permission from Bates *et al.* [41]. Copyright (2014) Elsevier.

Interpretation of such data is intrinsically complicated, since several different Cu species forming on the different stages of the reaction contribute to the signal. The common approach is to measure also the spectra of relevant reference materials, and, performing linear combination analysis, determine the relative contribution of each species to the spectrum of the catalyst under SCR conditions. Such strategy was adapted in the works of McEwen *et al.* [19] and Bates *et al.* [41], where samples with different Cu loadings were tested. Fitting the data with the Cu(I) and Cu(II) standards allowed to determine the ratio between the amounts of Cu species of these oxidation states during the reaction (figure 5).

The second strategy is to probe separately different stages of SCR reaction thus testing the independently developed hypotheses regarding the behavior of the active sites in particular conditions. Such approach allowed Janssens *et al.* to decouple the oxidation and reduction stages of the suggested SCR cycle [7]. In particular, the authors have tested the reducing capability of different agents, namely NO, NH_3 and their mixture (figure 6a). The results clearly indicate that almost complete reduction occurs only after exposure to the mixture of NO and NH_3. The resulting spectrum is characteristic for Cu(I) species in linear geometry [5]. Conversely, NO alone is not able to reduce Cu(II). Exposure to NH_3 leads only to a partial reduction accompanied by the formation of a linear Cu complex, while around 75% of Cu species remain oxidized, presumably forming tetrammine complexes (figure 6b,c), as observed by Janssens *et al.* [7]. Series of such *in situ* experiments with the components of SCR mixture allowed the authors to develop a feasible mechanism of the SCR reaction (scheme 1), where a key role is played by the nitrite-nitrate equilibrium, which has to be investigated in more detail in future spectroscopic studies.

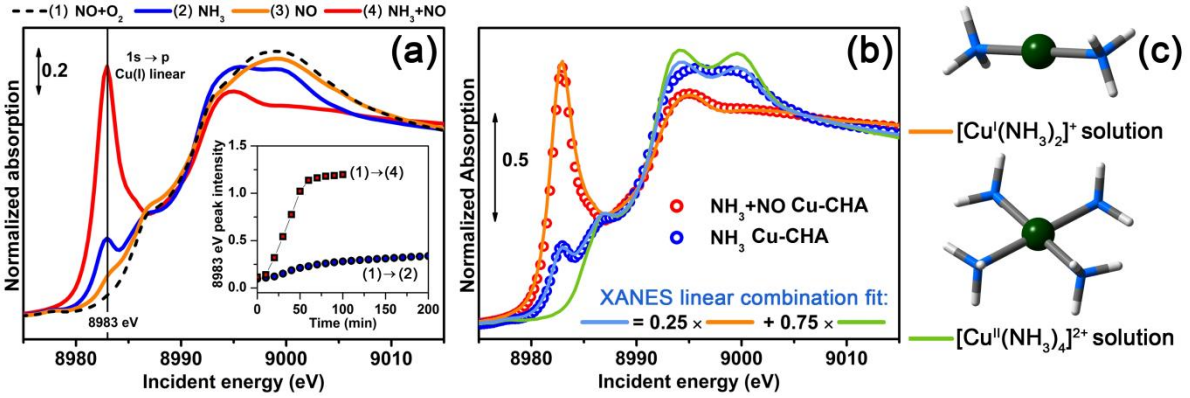

Figure 6. (a) *In situ* Cu K-edge XANES demonstrating the reducing capability at 200 °C of 1200 ppm NH_3 (2: blue curve), 1000 ppm NO (3: orange curve), and a mixture of 1200 ppm NH_3 + 1000 ppm NO (4: red curve) on the Cu(II) state obtained after initial oxidation in a mixture of 1000 ppm NO + 10% O_2 (a: dashed black curve). Inset: development of the intensity at 8983 eV with time with NH_3 only (1 → 2) and with a mixture of NH_3 + NO (1 → 4), visualizing the different reduction behavior with time in these cases. (b) Cu K-edge XANES spectra of the $[Cu^{I}(NH_3)_2]^+$ and $[Cu^{II}(NH_3)_4]^{2+}$ amino complexes (orange and green lines) compared with the data for Cu-SSZ-13 exposed to 1200 ppm NH_3 and 1200 ppm NH_3 + 1000 ppm NO at 200 °C (empty circles). Light-blue solid line corresponds to a linear combination of 25% $[Cu^{I}(NH_3)_2]^+$ and 75% $[Cu^{II}(NH_3)_4]^{2+}$. (c) Models of $[Cu^{I}(NH_3)_2]^+$ and $[Cu^{II}(NH_3)_4]^{2+}$ amino complexes. Color code: Cu – green; N – blue; H – white. Adapted with permission from Janssens *et al.* [7]. Copyright (2015) American Chemical Society.

Similar strategy of probing particular intermediate states of the reaction was adapted by Günter *et al.* who used XES and high-energy resolution fluorescence detected (HERFD) XANES for characterizing different stages of SCR reaction [42]. It was possible to detect the formation of Cu-N bond upon coordination of NH_3 monitoring the shift of Kβ" satellite from 8956.9 to 8958.3 eV (figure 7). Notably, no such shift was observed in the cases when NH_3 was absent from the feed, indicating thus the very weak coordination of NO to Cu accompanied by minor changes in Cu local environment.

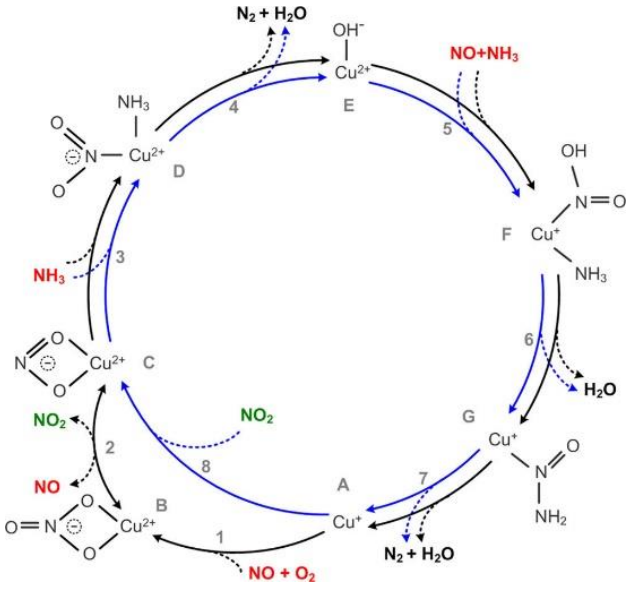

Scheme 1. Possible mechanism of SCR reaction. The fast SCR cycle is shown in blue, the NO activation cycle - in black. Reactants are indicated in red, reaction products - in black, and the NO_2 intermediate - in green. Reproduced with permission from Janssens et al. [7]. Copyright (2015) American Chemical Society.

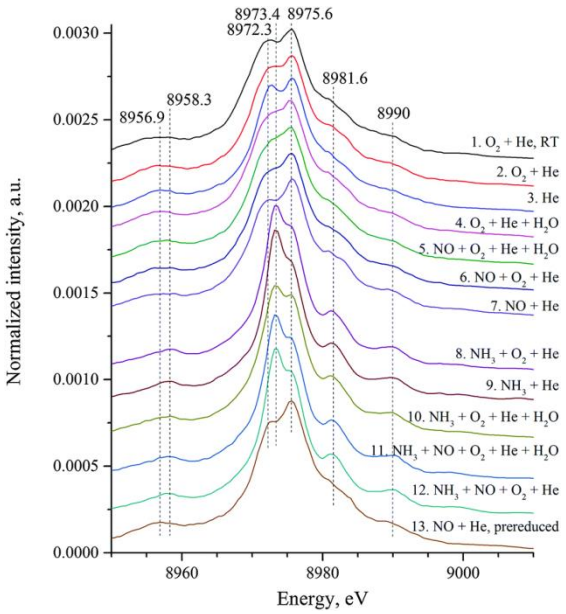

Figure 7. Cu valence-to-core ($K\beta_{2,5}$ and $K\beta''$) XES spectra of Cu-SSZ-13 catalyst in the course of the NH_3-SCR reaction and under exposure to the related model gas mixtures at 200 °C. Reproduced with permission from Günter et al. [42]. Copyright (2015) The Royal Society of Chemistry.

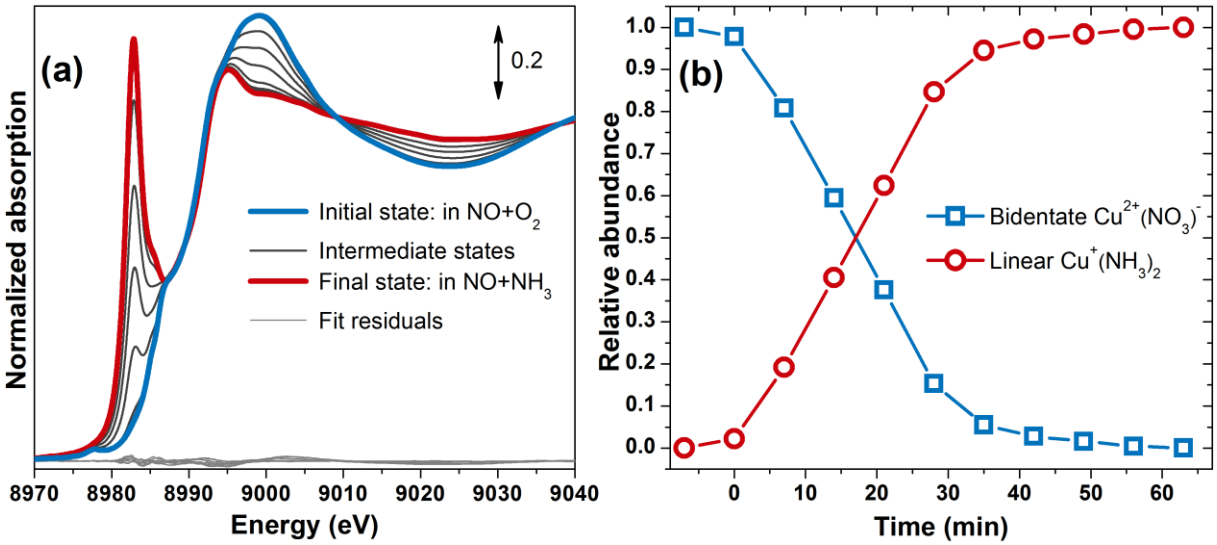

Figure 8. (a) Evolution of Cu K-edge XANES spectra of Cu-SSZ-13 after switching from 1000 ppm NO + 10% O_2 flux (initial state) to 1000 ppm NO + 1200 ppm NH_3 flux (intermediate states and final state) at 200 °C (b) Relative abundance of $Cu^{2+}(NO_3)^-$ bidentate nitrate and linear $Cu^+(NH_3)_2$ complex after changing the flux composition from $NO+O_2$ to $NO+NH_3$. The moment when the fluxes were switched and the measurement of the first "intermediate" spectrum was initiated corresponds to time 0. Each pair of points in panel (b) was obtained performing a linear combination fit of the corresponding intermediate spectrum presented in panel (a) considering the spectra of the initial and final states as standards. Unscaled residuals of all fits are presented in the bottom panel (a).

Two above mentioned approaches can certainly be combined in order to reach a better understanding of the SCR process. In particular, XANES linear combination studies at SCR conditions can be performed using as standards not the spectra of reference materials, but those of Cu-SSZ-13, collected at stable conditions, where the forming species are well-characterized. In such way more accurate quantitative data on the structure of active sites under real working conditions can be obtained. An *in situ* study of stored Cu-nitrates [7] reduction by NH_3 and NO in Cu-SSZ-13 presented in figure 8 serves to illustrate the possibilities of such approach. To the best of our knowledge these kind of studies in SCR conditions have not been reported yet, but surely will appear in the literature in the nearest future.

Notably, with the development of specialized computer codes, it has become possible to analyze the XANES data not only comparing the spectra with those of model compounds, but also simulating them directly for a given structural model. Due to the high porosity of the structure and significant anisotropy of Cu local environment, in case of Cu-SSZ-13 full potential codes are likely to be preferable to those that use the muffin-tin approximation and show excellent results for densely-packed systems [43]. The main drawback of full-potential codes is that usually they are up to two orders of magnitude slower than muffin-tin analogues, such as the most widely used FEFF code [44], and therefore require considerable computational resources. However, recently one of the mature full potential codes, FDMNES [45], was considerably sped-up due to the use of sparse matrices and dedicated solvers [46]. Decrease of calculation time by an order of 40 allowed to carry out studies which before were hardly feasible without huge computational clusters. To illustrate this, figure 9 summarizes the results of a structural investigation of the $[Cu(NH_3)_2]^+$ formed in CHA cavity upon the exposure of the material to the mixture of NH_3 and NO (figure 9a). The simulated spectrum of the DFT model showed an underestimated gap between the first two XANES maxima and therefore the Cu–N distances were decreased stepwise from the DFT value of 1.92 Å (figure 9b). The best agreement with the experiment was reached at Cu–N distance of 1.82 Å, which is significantly shorter compared to the DFT value (figure 9c). Total calculation time for each of the reported spectra was around 24 hours, which would mean more than a month and twice as much memory with the old version of FDMNES, clearly driving the current task out of the range of feasibility.

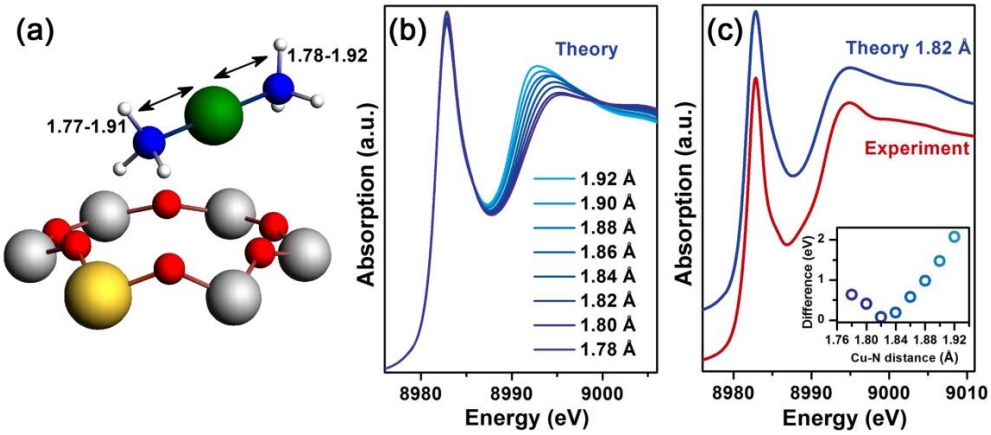

Figure 9. (a) Fragment of the structural model of $[Cu(NH_3)_2]^+$ complex in the large CHA cavity above the 6-ring. The variation range of the distances is shown in Å; (b) Theoretical spectra for different Cu–N distances; (c) Comparison of the best simulated spectrum to the experimental data collected at 200 °C in 1200 ppm NH_3 + 1000 ppm NO atmosphere. The inset shows the discrepancy of the experimental and theoretical values of the gap between the first two XANES maxima as a function of Cu–N distance.

4. Conclusion

Due to the efforts of many research groups, in the past five years there has been a marked advance in the understanding of the structure and reactivity of the active sites in Cu-SSZ-13 catalyst. As illustrated in this review, significant part of the insights were gained by the element-selective XAS/XES studies,

complemented by laboratory techniques and theoretical calculations. Since the first mechanisms of SCR reaction catalyzed by Cu-SSZ-13 were proposed [47-49], new XAS insights allowed to discard several seemingly plausible paths, such as Cu^{2+} reduction by NO alone, to characterize the active sites in the activated material and to shed light on the structure of the intermediate species. It allowed to develop a consistent scheme of the catalytic cycle respecting the stoichiometry and charge conservation, avoiding at the same time adsorption and desorption of molecular fragments and isolated ions [7]. Nonetheless, there is undoubtedly still a lot to discover in the further studies, particularly (but not exclusively) exploring the formation of Cu nitrates and nitrites, checking the influence of Cu/Al and Si/Al ratios on the structures that form in Cu-SSZ-13 at different conditions, quantifying the Cu speciation in SCR conditions at different temperatures. We foresee that the role of XAS and XES spectroscopy in solving these open questions will be of particular importance.

Acknowledgments
The authors are strongly indebted to the Haldor Topsøe team involved in the SCR catalysis (T.V.W. Janssens, H. Falsig, L.F. Lundegaard, P.N.R. Vennestrøm, S.B. Rasmussen, P.G. Moses), to A. Godiksen and S. Mossin (from DTU) and to F. Giordanino (Turin University), for an outstanding 4-years collaboration on the subject. K.A.L., C.L. and A.V.S. acknowledge the megagrant of the Russian Federation Government to support scientific research at the Southern Federal University, no. 14.Y26.31.0001.

References
[1] Zones S I 1985 U.S. Patent 4544538
[2] Kwak J H, Tonkyn R G, Kim D H, Szanyi J and Peden C H F 2010 *J. Catal.* **275** 187-90
[3] Kwak J H, Tran D, Burton S D, Szanyi J, Lee J H and Peden C H F 2012 *J. Catal.* **287** 203-9
[4] Beale A M, Gao F, Lezcano-Gonzalez I, Peden C H F and Szanyi J 2015 *Chem. Soc. Rev.* **44** 7371-405
[5] Giordanino F, Borfecchia E, Lomachenko K A, Lazzarini A, Agostini G, Gallo E, Soldatov A V, Beato P, Bordiga S and Lamberti C 2014 *J. Phys. Chem. Lett.* **5** 1552-9
[6] Borfecchia E, Lomachenko K A, Giordanino F, Falsig H, Beato P, Soldatov A V, Bordiga S and Lamberti C 2015 *Chem. Sci.* **6** 548-63
[7] Janssens T V W *et al.* 2015 *ACS Catal.* **5** 2832-45
[8] Doronkin D E, Casapu M, Günter T, Müller O, Frahm R and Grunwaldt J D 2014 *J. Phys. Chem.* C **118** 10204-12
[9] Boubnov A, Carvalho H W P, Doronkin D E, Günter T, Gallo E, Atkins A J, Jacob C R and Grunwaldt J D 2014 *J. Am. Chem. Soc.* **136** 13006-15
[10] Bordiga S, Groppo E, Agostini G, van Bokhoven J A and Lamberti C 2013 *Chem. Rev.* **113** 1736-850
[11] Van Bohkoven J A and Lamberti C 2016 X-ray absorption and emission spectroscopy for catalysis *X-Ray Absorption and X-ray Emission Spectroscopy: Theory and Applications* vol 2 eds van Bokhoven J A and Lamberti C (New York: John Wiley & Sons) pp 353-83.
[12] Soldatov A V and Lomachenko K A 2016 Nanostructured Materials *X-Ray Absorption and X-ray Emission Spectroscopy: Theory and Applications* vol 2 eds van Bokhoven J A and Lamberti C (New York: John Wiley & Sons) pp 809-27.
[13] Pluth J J, Smith J V and Mortier W J 1977 *Mat. Res. Bull.* **12** 1001-7
[14] Bull I, Boorse R S, Jaglowski W M, Koermer G S, Moini A, Patchett J A, Xue W M, Burk P, Dettling J C and Caudle M T 2008 U.S. Patent 20080226545
[15] Fickel D W and Lobo R F 2010 *J. Phys. Chem.* C **114** 1633-40
[16] Korhonen S T, Fickel D W, Lobo R F, Weckhuysen B M and Beale A M 2011 *Chem. Commun.* **47** 800-2
[17] Pierloot K, Delabie A, Groothaert M H and Schoonheydt R A 2001 *Phys. Chem. Chem. Phys.* **3** 2174-83

[18] Deka U, Juhin A, Eilertsen E A, Emerich H, Green M A, Korhonen S T, Weckhuysen B M and Beale A M 2012 *J. Phys. Chem.* C **116** 4809-18
[19] McEwen J S, Anggara T, Schneider W F, Kispersky V F, Miller J T, Delgass W N and Ribeiro F H 2012 *Catal. Today* **184** 129-44
[20] Kwak J H, Varga T, Peden C H F, Gao F, Hanson J C and Szanyi J 2014 *J. Catal.* **314** 83-93
[21] Cheung T, Bhargava S K, Hobday M and Foger K 1996 *J. Catal.* **158** 301-10
[22] Keith Hall W and Valyon J 1992 *Catal. Lett.* **15** 311-5
[23] Jang H J, Keith Hall W and d'Itri J L 1996 *J. Phys. Chem.* **100** 9416-20
[24] Li Y and Keith Hall W 1991 *J. Catal.* **129** 202-15
[25] Sarkany J, d'Itri J L and Sachtler W M H 1992 *Catal. Lett.* **16** 241-9
[26] Valyon J and Keith Hall W 1993 *J. Phys. Chem.* **97** 1204-12
[27] Turnes Palomino G, Fisicaro P, Bordiga S, Zecchina A, Giamello E and Lamberti C 2000 *J. Phys. Chem.* B **104** 4064-73
[28] Llabrés i Xamena F X, Fisicaro P, Berlier G, Zecchina A, Turnes Palomino G, Prestipino C, Bordiga S, Giamello E and Lamberti C 2003 *J. Phys. Chem.* B **107** 7036-44
[29] Giordanino F, Vennestrom P N R, Lundegaard L F, Stappen F N, Mossin S, Beato P, Bordiga S and Lamberti C 2013 *Dalton Trans.* **42** 12741-61
[30] Godiksen A, Stappen F N, Vennestrom P N R, Giordanino F, Rasmussen S B, Lundegaard L F and Mossin S 2014 *J. Phys. Chem.* C **118** 23126-38
[31] Andersen C W, Bremholm M, Vennestrom P N R, Blichfeld A B, Lundegaard L F and Iversen B B 2014 *IUCrJ* **1** 382-6
[32] Alayon E M C, Nachtegaal M, Bodi A and van Bokhoven J A 2014 *ACS Catal.* **4** 16-22
[33] Ene A B, Bauer M, Archipov T and Roduner E 2010 *Phys. Chem. Chem. Phys.* **12** 6520-31
[34] Groothaert M H, Smeets P J, Sels B F, Jacobs P A and Schoonheydt R A 2005 *J. Am. Chem. Soc.* **127** 1394-5
[35] Groothaert M H, van Bokhoven J A, Battiston A A, Weckhuysen B M and Schoonheydt R A 2003 *J. Am. Chem. Soc.* **125** 7629-40
[36] Lamberti C, Spoto G, Scarano D, Paze C, Salvalaggio M, Bordiga S, Zecchina A, Palomino G T and Dacapito F 1997 *Chem. Phys. Lett.* **269** 500-8
[37] Grundner S, Markovits M A C, Li G, Tromp M, Pidko E A, Hensen E J M, Jentys A, Sanchez-Sanchez M and Lercher J A 2015 *Nat. Commun.* **6**
[38] Woertink J S, Smeets P J, Groothaert M H, Vance M A, Sels B F, Schoonheydt R A and Solomon E I 2009 *Proc. Natl. Acad. Sci. U. S. A.* **106** 18908-13
[39] Alayon E M C, Nachtegaal M, Bodi A, Ranocchiari M and van Bokhoven J A 2015 *Phys. Chem. Chem. Phys.* **17** 7681-93
[40] Kispersky V F, Kropf A J, Ribeiro F H and Miller J T 2012 *Phys. Chem. Chem. Phys.* **14** 2229-38
[41] Bates S A, Verma A A, Paolucci C, Parekh A A, Anggara T, Yezerets A, Schneider W F, Miller J T, Delgass W N and Ribeiro F H 2014 *J. Catal.* **312** 87-97
[42] Günter T, Carvalho H W P, Doronkin D E, Sheppard T, Glatzel P, Atkins A J, Rudolph J, Jacob C R, Casapu M and Grunwaldt J D 2015 *Chem. Commun.* **51** 9227-30
[43] Rehr J J and Albers R C 2000 *Rev. Mod. Phys.* **72** 621-54
[44] Rehr J J, Kas J J, Vila F D, Prange M P and Jorissen K 2010 *Phys. Chem. Chem. Phys.* **12** 5503-13
[45] Joly Y 2001 *Phys. Rev.* B **63** 125120
[46] Guda S A *et al.* 2015 *J. Chem. Theory Comput.* **11** 4512-21
[47] Gao F, Kwak J H, Szanyi J and Peden C H F 2013 *Top. Catal.* **56** 1441-59
[48] Kwak J H, Lee J H, Burton S D, Lipton A S, Peden C H F and Szanyi J 2013 *Angew. Chem. Int. Ed.* **52** 9985-9
[49] Paolucci C, Verma A A, Bates S A, Kispersky V F, Miller J T, Gounder R, Delgass W N, Ribeiro F H and Schneider W F 2014 *Angew. Chem. Int. Ed.* **53** 11828-33